J. Fluid Mech. (1999), *vol.* 391, *pp.* 45–65. Printed in the United Kingdom

Long interfacial waves in multilayer thin films and coupled Kuramoto–Sivashinsky equations

By IGOR L. KLIAKHANDLER†

School of Mathematical Sciences, Tel-Aviv University,
Tel-Aviv 69978, Israel

(Received 6 January 1998 and in revised form 1 February 1999)

The coupled Kuramoto–Sivashinsky (CKS) equations for multilayer downflowing films are derived and explored. The CKS equations exhibit a wealth of dynamical behaviour, displaying travelling periodic waves, regular and chaotic-like patterns, coexistence of different attractors, and perfect and imperfect synchronization of the interfaces. New physical effects are found, such as suppression of the Rayleigh–Taylor instability for heavy-top stratified films, and new surface-tension-driven instability.

1. Introduction

The downflowing homogeneous viscous film is one of the most graphic and experimentally accessible examples of an intrinsically unstable extended system. The flow has attracted much attention due to its conceptual simplicity, rich dynamical phenomenology, and technological relevance (see review papers by Lin 1983*a* and Chang 1994). Related interfacial flows were surveyed in a monograph by Joseph & Renardy (1993).

The basic result of Mei (1966) is that the medium-amplitude waves in creeping film flows are described by the Burgers equation,

$$h_\tau + hh_\xi = h_{\xi\xi}. \tag{1}$$

Here $h(\xi,\tau) \sim H(x,t) - 1$ is the rescaled deviation of the interface H from its steady-state location 1, and ξ and τ are the scaled downstream coordinate and time, respectively.

The impact of inertia and surface tension leads to a new physics. The film flow becomes susceptible to long-wavelength instability due to inertia (Benjamin 1957; Yih 1963). Surface tension damps short-wavelength modes. Nepomnyashchy (1974) and Homsy (1974) derived the equation governing the interfacial dynamics of homogeneous films in the limiting case of large surface tension. This equation has appeared further in many physical contexts such as drift waves in plasma (Cohen *et al.* 1976), spatial patterns in chemical oscillations (Kuramoto & Tsuzuki 1976), unstable flame fronts (Sivashinsky 1977), and other interfacial problems (Hooper & Grimshaw 1985; Shlang *et al.* 1985). The equation is known today as the Kuramoto–Sivashinsky (KS) equation

$$h_\tau + hh_\xi + h_{\xi\xi} + h_{\xi\xi\xi\xi} = 0. \tag{2}$$

† Current address: Department of Mathematics, Lawrence Berkeley National Laboratory, Mail Stop 50A-2152, 1 Cyclotron Road, Berkeley, CA 94720, USA. E-mail: igork@math.lbl.gov.

The KS equation has enjoyed much attention due to its ability to display turbulence-like behaviour (see the review paper by Cross & Hohenberg 1993, with further references).

Multiple-layer stratified viscous films constitute a natural generalization of a homogeneous film. Such films are encountered in wood stacks in cooling towers, evaporators, density currents, liquid extraction, and on wetted-wall pollutant absorbers and scrubbers. In oil transportation, the thin films are used as lubricant layers. A model of multilayer film flow has been used in geophysical problems to decipher the generation of transverse ridges occurring on the surfaces of rock glacier forms. An especially important application of multilayer liquid films is in the precision coating of colour photographic films and papers, which often involve more than 10 different layers. In chemical technology the interfacial waves enhance the transport of mass, heat and momentum across the film, whereas formation of the waves in coating layers is highly undesirable.

Linear stability analysis of multilayer film flows has been addressed in a number of papers (Kao 1965*a*, *b*, 1968; Akhtaruzzaman, Wang & Lin 1978; Wang, Seaborg & Lin 1978; Lin 1983*b*; Loewenherz & Lawrence 1989; Weinstein & Kurz 1991; Chen 1993; Kobayashi 1992, 1995). In the recent experiments by Kurz, Weinstein & Ruschak (1994) and Kobayashi (1995) the growing unstable modes and nonlinear waves in multilayer films were identified and described.

Kliakhandler & Sivashinsky (1997) studied the nonlinear dynamics of creeping multilayer film flows and extended the result of Mei, equation (1), to coupled Burgers equations. It turns out that the presence of additional interfaces and the corresponding coupling of the equations lead to new instabilities and patterns unfeasible in the single Burgers equation (1).

Inertia, unstable density stratification, and surface tension lead to the single KS equation in homogeneous film and two-layer Couette and Poiseuille flows. It is reasonable to expect that in *multilayer* film flows these ingredients will lead to coupled KS equations, where the coupling will result in a wealth of new interesting nonlinear dynamical behaviour.

The objective of the present work is to derive and to study the coupled Kuramoto–Sivashinsky (CKS) equations for multiple-layer stratified film flows.

2. Statement of the problem

Consider a two-dimensional multiple-layer stratified film of incompressible Newtonian liquids, involving n layers with viscosities μ_1, μ_2, etc. and densities ρ_1, ρ_2, etc. flowing down an inclined plane, figure 1. The associated steady-state planar interfaces are marked as H_1^0, H_2^0, etc. The surrounding atmosphere is assumed to be a weightless, inviscid quiescent gas.

In terms of dimensionless variables (defined below), the flow equations are

$$\frac{\partial u_i}{\partial x} + \frac{\partial v_i}{\partial y} = 0, \tag{3}$$

$$R\left(\frac{\partial u_i}{\partial t} + u_i\frac{\partial u_i}{\partial x} + v_i\frac{\partial u_i}{\partial y}\right) = 2 - \frac{2}{r_i}\frac{\partial p_i}{\partial x} + \frac{m_i}{r_i}\left(\frac{\partial^2 u_i}{\partial x^2} + \frac{\partial^2 u_i}{\partial y^2}\right), \tag{4}$$

$$R\left(\frac{\partial v_i}{\partial t} + u_i\frac{\partial v_i}{\partial x} + v_i\frac{\partial v_i}{\partial y}\right) = -2\cot\theta - \frac{2}{r_i}\frac{\partial p_i}{\partial y} + \frac{m_i}{r_i}\left(\frac{\partial^2 v_i}{\partial x^2} + \frac{\partial^2 v_i}{\partial y^2}\right). \tag{5}$$

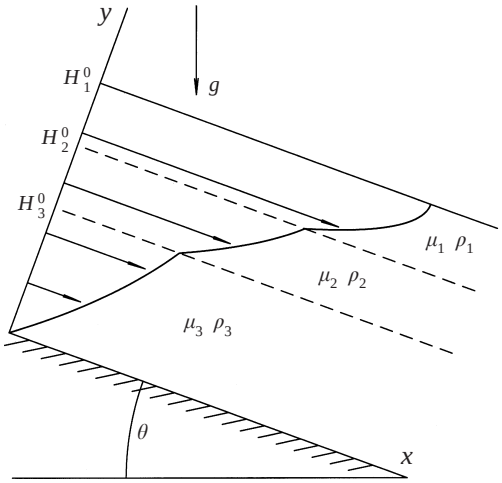

FIGURE 1. Geometry of a multilayer downflowing film.

Here x, y are the streamwise and spanwise coordinates, respectively, in units of the unperturbed total film thickness d; u, v are the corresponding velocity components, referred to $\overline{U} = gd^2\rho_1 \sin\theta/2\mu_1$, where g is the gravitational acceleration, p_i is the pressure in the ith layer in units of $\rho_1 gd \sin\theta$, t is the time referred to $d/\overline{U}$; the index $i = 1, 2, \ldots, n$ marks the first $H_2 < y < H_1$, second $H_3 < y < H_2, \ldots$, nth $0 < y < H_n$ layers respectively, where $H_i(x, t)$ is the ith interface locus; $m_i = \mu_i/\mu_1$ and $r_i = \rho_i/\rho_1$ are the ratios of viscosity and density, respectively; $R = \overline{U}d\rho_1/\mu_1 = gd^3\rho_1^2 \sin\theta/2\mu_1^2$ is the Reynolds number.

The interface boundary conditions are expressed in the terms of the normal $\boldsymbol{n}_i$ and curvature S_i of the ith interface H_i, and the stress tensor $\boldsymbol{T}_j$ of the jth layer $(j = i - 1, i)$:

$$\boldsymbol{n}_i = \frac{1}{\sqrt{1 + \left(\partial H_i/\partial x\right)^2}}(-\partial H_i/\partial x, 1), \quad S_i = \frac{\partial H_i^2/\partial x^2}{(1 + \left(\partial H_i/\partial x\right)^2)^{3/2}}, \tag{6}$$

$$\boldsymbol{T}_j = \begin{pmatrix} m_j \dfrac{\partial u_j}{\partial x} - p_j & \dfrac{m_j}{2}\left(\dfrac{\partial u_j}{\partial y} + \dfrac{\partial v_j}{\partial x}\right) \\ \dfrac{m_j}{2}\left(\dfrac{\partial u_j}{\partial y} + \dfrac{\partial v_j}{\partial x}\right) & m_j \dfrac{\partial v_j}{\partial y} - p_j \end{pmatrix} \tag{7}$$

(there is no summation here over indices).

On the bottom $y = 0$, at the free surface $y = H_1(x, t)$ and at the inner interfaces $y = H_i(x, t)$, $i = 2, 3, \ldots, n$, the following boundary conditions are imposed:

$$u_n = v_n = 0 \quad \text{at} \quad y = 0, \tag{8}$$

$$u_{i-1} = u_i, \quad v_{i-1} = v_i \quad \text{at} \quad y = H_i, \quad i = 2, 3, \ldots, n, \tag{9}$$

$$\boldsymbol{T}_{i-1} \cdot \boldsymbol{n}_i = \boldsymbol{T}_i \cdot \boldsymbol{n}_i - W\gamma_i S_i \boldsymbol{n}_i \quad \text{at} \quad y = H_i, \quad i = 2, 3, \ldots, n, \tag{10}$$

$$\boldsymbol{T}_1 \cdot \boldsymbol{n}_1 = p_0 \boldsymbol{n}_1 - W S_1 \boldsymbol{n}_1 \quad \text{at} \quad y = H_1, \tag{11}$$

$$\frac{\partial H_i}{\partial t} + u_i \frac{\partial H_i}{\partial x} - v_i = 0 \quad \text{at} \quad y = H_i, \quad i = 1, 2, \ldots, n. \tag{12}$$

Here $\gamma_i = W_i/W_1$ is the surface tension ratio, where W_i is the dimensionless surface tension (Weber number) at the ith interface in units of $\rho_1 g d^2 \sin\theta$; $W = W_1 = \rho_1 g d^2 \sin\theta$ is chosen as a typical surface tension; $p_0 = \text{const.}$ is the atmosphere pressure. Relations (8)–(12) imply the no-slip condition at the bottom plane, the continuity of the velocity and continuity of the stress at the inner interfaces, continuity of the stress at the outer interface, and impermeability of the interfaces (kinematic boundary conditions), respectively.

Employing continuity equation (3) and boundary conditions (8), (9), the kinematic boundary conditions (12) may be represented in a divergent form of the conservation laws,

$$\frac{\partial H_i}{\partial t} + \frac{\partial}{\partial x}\sum_{k=i}^{n} I_k = 0, \quad I_k = \int_{H_{k+1}}^{H_k} u_k \, \mathrm{d}y. \tag{13}$$

Here I_k is the volumetric flow rate between kth and $(k+1)$th interface, where $H_{n+1} = 0$ corresponds to the rigid wall.

Equations (3)–(5) jointly with the interfacial conditions (8)–(11) and (13) constitute a free-boundary problem for $H_i(x,t)$, $i = 1, 2, \ldots, n$.

3. Derivation of coupled Benney and coupled Kuramoto–Sivashinsky equations

To clarify the derivation of the CKS equations, I outline the conventional techniques for derivation of the single KS equation for a homogeneous film.

The Reynolds number of the flow is assumed to be not too large, i.e. the lubrication approximation is used. The case of relatively large Reynolds numbers may be described in terms of the boundary layer approximation which is not considered here (see review paper of Chang 1994, with further references).

The single KS equation may be derived by the multi-scale asymptotic expansions following Nepomnyashchy (1974). Linear stability analysis yields the range of parameters where the downflowing film is susceptible to long-wavelength instability. Near the stability threshold the interfacial waves are expected to be small amplitude and slowly varying in both time and space. The typical length scale of the waves therefore significantly exceeds the thickness of the film, and one can separate the variables of the problem along and across the film. As a result, one obtains the KS equation directly in terms of the interface locus.

The single KS equation may also be extracted from the equation derived by Benney (1966). In this approach, the wave slopes are assumed to be small whereas the wave amplitudes are arbitrary. The long-wavelength, or gradient, asymptotic expansion leads to the strongly nonlinear equation for the interface evolution. The shortened version of the original Benney equation, dominated by strong surface tension, acquires the form

$$\frac{\partial H}{\partial t} + \frac{\partial}{\partial x}\left[\tfrac{2}{3}H^3 + \left(\tfrac{8}{15}RH^6 - \tfrac{2}{3}H^3\right)\frac{\partial H}{\partial x} + \tfrac{2}{3}WH^3\frac{\partial^3 H}{\partial x^3}\right] = 0. \tag{14}$$

Here $H(x,t)$ is the locus of the film interface. The weakly nonlinear limit of the Benney equation (14) for $W \gg 1$ (combined with transition to a special reference frame) leads to the KS equation. This procedure was first used by Homsy (1974). Note that Burgers equation (1) may also be recovered as a special case of the Benney equation (14).

Both procedures may be applied to multilayer films to derive the CKS equations. In the present work, the CKS equations are derived through the coupled Benney equations. The reasons are that (i) the coupled Benney equations are themselves expected to be an interesting dynamical model and a source of other models, and (ii) all special cases may be extracted directly from the coupled Benney equations, whereas the application of asymptotic expansions formally requires one to repeat the whole derivation for each new kind of instability.

The derivation is straightforward but quite long. I therefore display the principal steps of the procedure and present the final result, omitting the tedious algebra involved.

One assumes that the typical surface tension W is large, $W \gg 1$; all interfacial tensions are of the same order, i.e. $\gamma_i \simeq O(1)$ for all i. This ensures that the surface tension effects are retained in the leading-order approximation.

Introduce the small parameter $\varepsilon \ll 1$ (akin to the shallow water parameter), and the following scaled variables:

$$\xi = \varepsilon x, \quad \eta = y, \quad \tau = \varepsilon t, \tag{15}$$

$$U_i = u_i, \quad V_i = \varepsilon^{-1} v_i, \quad P_i = p_i, \quad \Omega = \varepsilon^2 W. \tag{16}$$

In the new variables, the flow equations (3)–(5) acquire the following form:

$$\frac{\partial U_i}{\partial \xi} + \frac{\partial V_i}{\partial \eta} = 0, \tag{17}$$

$$\varepsilon R\left(\frac{\partial U_i}{\partial \tau} + U_i \frac{\partial U_i}{\partial \xi} + V_i \frac{\partial U_i}{\partial \eta}\right) = 2 - \varepsilon \frac{2}{r_i}\frac{\partial P_i}{\partial \xi} + \frac{m_i}{r_i}\left(\varepsilon^2 \frac{\partial^2 U_i}{\partial \xi^2} + \frac{\partial^2 U_i}{\partial \eta^2}\right), \tag{18}$$

$$\varepsilon^2 R\left(\frac{\partial V_i}{\partial \tau} + U_i \frac{\partial V_i}{\partial \xi} + V_i \frac{\partial V_i}{\partial \eta}\right) = -2\cot\theta - \frac{2}{r_i}\frac{\partial P_i}{\partial \eta} + \frac{m_i}{r_i}\left(\varepsilon^3 \frac{\partial^2 V_i}{\partial \xi^2} + \varepsilon \frac{\partial V_i}{\partial \eta}\right). \tag{19}$$

The boundary conditions (8)–(11) become

$$U_n = V_n = 0 \quad \text{at} \quad \eta = 0, \tag{20}$$

$$U_{i-1} = U_i, \quad V_{i-1} = V_i \quad \text{at} \quad \eta = H_i, \quad i = 2, 3, \ldots, n, \tag{21}$$

$$\boldsymbol{T}_{i-1} \cdot \boldsymbol{n}_i = \boldsymbol{T}_i \cdot \boldsymbol{n}_i - \Omega \gamma_i S_i \boldsymbol{n}_i \quad \text{at} \quad \eta = H_i, \quad i = 2, 3, \ldots, n, \tag{22}$$

$$\boldsymbol{T}_1 \cdot \boldsymbol{n}_1 = P_0 \boldsymbol{n}_1 - \Omega S_1 \boldsymbol{n}_1 \quad \text{at} \quad \eta = H_1, \tag{23}$$

$$\frac{\partial H_i}{\partial \tau} + \frac{\partial}{\partial \xi}\sum_{k=i}^{n} I_k = 0, \quad I_k = \int_{H_{k+1}}^{H_k} U_k \, \mathrm{d}\eta, \tag{24}$$

where now

$$\boldsymbol{n}_i = \frac{1}{\sqrt{1 + \varepsilon^2 \left(\partial H_i / \partial \xi\right)^2}}(-\varepsilon \partial H_i / \partial \xi, 1), \quad S_i = \frac{\partial H_i^2 / \partial \xi^2}{(1 + \varepsilon^2 \left(\partial H_i / \partial \xi\right)^2)^{3/2}}, \tag{25}$$

$$\boldsymbol{T}_j = \begin{pmatrix} \varepsilon m_j \dfrac{\partial U_j}{\partial \xi} - P_j & \dfrac{m_j}{2}\left(\dfrac{\partial U_j}{\partial \eta} + \varepsilon^2 \dfrac{\partial V_j}{\partial \xi}\right) \\ \dfrac{m_j}{2}\left(\dfrac{\partial U_j}{\partial \eta} + \varepsilon^2 \dfrac{\partial V_j}{\partial \xi}\right) & \varepsilon m_j \dfrac{\partial V_j}{\partial \eta} - P_j \end{pmatrix}. \tag{26}$$

The velocity and pressure in the layers are sought as asymptotic expansions in ε,

$$(U_i, V_i, P_i) = (U_i^{(0)}, V_i^{(0)}, P_i^{(0)}) + \varepsilon(U_i^{(1)}, V_i^{(1)}, P_i^{(1)}) + \varepsilon^2(U_i^{(2)}, V_i^{(2)}, P_i^{(2)}) + \cdots . \tag{27}$$

Here $(U_i^{(0)}, V_i^{(0)}, P_i^{(0)})$ correspond to the basic steady-state unidirectional flow. This approach leads to a hierarchy of successive approximations.

The zeroth-order problem yields

$$\frac{\partial H_i}{\partial \tau} + \frac{\partial Q_i}{\partial \xi} = 0, \quad \text{or} \quad \frac{\partial H_i}{\partial t} + \frac{\partial Q_i}{\partial x} = 0. \tag{28}$$

Functions $Q_i(H_1, H_2)$ for two-layer film flows are presented in the Appendix. When the two-layer film degenerates to the homogeneous film, (28) reduce to a single leading-order equation for a homogeneous film,

$$\frac{\partial H}{\partial t} + \frac{\partial Q}{\partial x} = 0, \quad Q = \tfrac{2}{3}H^3. \tag{29}$$

The first-order expansion results in

$$\frac{\partial H_i}{\partial \tau} + \frac{\partial Q_i}{\partial \xi} + \varepsilon \frac{\partial}{\partial \xi}\left[\left(\cot\theta\ G_{ij} + RT_{ij}\right)\frac{\partial H_j}{\partial \xi} + \Omega F_{ij}\frac{\partial^3 H_j}{\partial \xi^3}\right] = 0. \tag{30}$$

Here the sum convention for repeated indices is adopted. The matrices G_{ij}, T_{ij}, F_{ij} are associated with the buoyancy, inertia, and surface tension impact, respectively. For two-layer flow, these matrices are presented in the Appendix. Similarly to the Benney equation (14), Q_i, G_{ij} and F_{ij} are homogeneous polynomials of third order with respect to $H_1, \ldots, H_n$, and T_{ij} are homogeneous polynomials of sixth order.

Equations (30) may be recast into the coupled Benney equations in the original variables,

$$\frac{\partial H_i}{\partial t} + \frac{\partial}{\partial x}\left[Q_i + \left(\cot\theta\ G_{ij} + RT_{ij}\right)\frac{\partial H_j}{\partial x} + WF_{ij}\frac{\partial^3 H_j}{\partial x^3}\right] = 0. \tag{31}$$

If the multilayer flow degenerates to the flow of a homogeneous film, e.g. for two-layer system $H_2 = 0$, or $H_2 = H_1$, or $r_2 = m_2 = 1$, the coupled Benney equations (31) reduce to the single Benney equation (14).

Weakly nonlinear approximation of (31) leads to the CKS equations:

$$\frac{\partial h_i}{\partial t} + \alpha_{ij}\frac{\partial h_j}{\partial x} + \beta_{ijk}\frac{\partial h_j h_k}{\partial x} + \left(\cot\theta\ \vartheta_{ij} + R\sigma_{ij}\right)\frac{\partial^2 h_j}{\partial x^2} + W\chi_{ij}\frac{\partial^4 h_j}{\partial x^4} = 0. \tag{32}$$

Here

$$h_i(x,t) = H_i - H_i^0, \tag{33}$$

$$\alpha_{ij} = \frac{\partial Q_i}{\partial H_j}(1, H_2^0, \ldots, H_n^0), \quad \beta_{ijk} = \frac{1}{2}\frac{\partial^2 Q_i}{\partial H_j \partial H_k}(1, \ldots, H_n^0), \tag{34}$$

$$\vartheta_{ij} = G_{ij}(1, \ldots, H_n^0), \quad \sigma_{ij} = T_{ij}(1, \ldots, H_n^0), \quad \chi_{ij} = F_{ij}(1, \ldots, H_n^0), \tag{35}$$

$$i, j, k = 1, 2, \ldots, n, \tag{36}$$

with h_i being the perturbations of the planar undisturbed interfaces H_i^0, figure 1. The constant tensors $\alpha_{ij}, \beta_{ijk}, \vartheta_{ij}, \sigma_{ij}, \chi_{ij}$ are determined by the basic unidirectional steady flow, i.e. by the distribution of viscosities μ_i, densities ρ_i, layer widths H_i^0, and interfacial tensions W_i. The concrete numerical values of the tensors are evaluated using the *Mathematica* software.

Equations (32) are the subject of the further study. They incorporate kinetic $\alpha_{ij}\partial h_j/\partial x$, buoyancy $\vartheta_{ij}\partial^2 h_j/\partial x^2$, inertia $\sigma_{ij}\partial^2 h_j/\partial x^2$, surface tension $\chi_{ij}\partial^4 h_j/\partial x^4$, and nonlinear $\beta_{ijk}\partial h_j h_k/\partial x$ effects. The single-interface counterpart of (32) is the single KS equation in a *quiescent* coordinate frame.

The mean drift of interfacial disturbances in the single KS equation (2) may be eliminated by transition to the special reference frame. However, this elimination cannot be done for the CKS equations (32) in multilayer films. The reason is that the eigenvalues of the matrix α_{ij} are different, in general. As a result, the interfaces are strongly coupled. This leads to new dynamic phenomena unfeasible in the flow of homogeneous film.

Note that unstable density stratification and inertia are expected to induce destabilizing effects in the long-wavelength range whereas surface tension provides damping of short-wavelength modes. Growth of unstable long-wavelength modes in (32) should be restrained by the nonlinear quadratic term. As a result, (32) are expected to be well-behaved dynamically.

In the case of a stabilizing density stratification, examined by Kliakhandler & Sivashinsky (1997), the interfacial dynamics of a multilayer system may be captured by simpler model. Formally, this situation may be described by truncation of (32),

$$\frac{\partial h_i}{\partial t} + \alpha_{ij}\frac{\partial h_j}{\partial x} + \beta_{ijk}\frac{\partial h_j h_k}{\partial x} + \cot\theta\ \vartheta_{ij}\frac{\partial^2 h_j}{\partial x^2} = 0. \tag{37}$$

Short-wavelength modes in (37) are damped due to stabilizing density stratification.

Equations (37) exhibit instability of so-called alpha-effect type, arising due to appearance of complex eigenvalues of matrix α_{ij}. This kind of instability may occur for (32) as well. The general contribution of the alpha-effect to the behaviour of (32) may be understood from model (37) (cf. Kliakhandler & Sivashinsky 1997). The possible dynamical responses of the full equations (32) in the case of the alpha-effect are not discussed here.

A few shortened versions of (32) are further explored to elucidate the role of surface tension, unstable buoyancy stratification, and inertia terms.

4. The surface-tension-driven instability

Consider vertical creeping film flow where the impact of surface tension may be studied in its simplest form. In this case the buoyancy and inertia terms drop out from the governing equations (32), resulting in

$$\frac{\partial h_i}{\partial t} + \alpha_{ij}\frac{\partial h_j}{\partial x} + \beta_{ijk}\frac{\partial h_j h_k}{\partial x} + W\chi_{ij}\frac{\partial^4 h_j}{\partial x^4} = 0. \tag{38}$$

A numerical check shows that the eigenvalues of the matrix χ_{ij} are always positive and real. Surface tension therefore suppresses the short-wavelength modes. As a result the system (38) is quite well-behaved.

To explore the dynamical properties of (38), scrutinize the linear stability problem as a first step. One assumes that the eigenvalues of the matrix α_{ij} are real. Set

$$h_i = a_i \exp\left[\mathrm{i}(kx - \omega t)\right], \tag{39}$$

with k being the real wavenumber and ω being the complex frequency. One considers therefore the ensuing stability problem in its temporal form. Substitution of (39) into the linearized (38) leads to the following eigenvalue problem:

$$\mathrm{i}\omega a_i = (\mathrm{i}k\alpha_{ij} + Wk^4\chi_{ij})a_j. \tag{40}$$

The truncated eigenvalue problem of (40), $\omega a_i = k\alpha_{ij}a_j$, ends up with pure real solutions $\omega_m = k\lambda_m^{(\alpha)}$, $m = 1,\ldots,n$. Here $\lambda_m^{(\alpha)}$ are real eigenvalues of the matrix α_{ij}. To clarify the impact of surface tension, write the next term of the long-wavelength expansion of relation (40),

$$\omega_m = k\lambda_m^{(\alpha)} + \mathrm{i}k^4 L_m, \quad m = 1,\ldots,n. \tag{41}$$

Here the constants L_m are defined by both matrices α_{ij} and χ_{ij},

$$L_m \equiv \mathscr{L}(\alpha_{ij},\chi_{ij})_m = \frac{\sum_{i,j=1}^{n}(-1)^{i+j}\chi_{ij}M_{ij}^{(\alpha)} + \lambda_m^{(\alpha)}\ \mathrm{tr}\ \chi_{ij}}{\mathrm{tr}\ \alpha_{ij} - n\lambda_m^{(\alpha)}}. \tag{42}$$

Here $M_{pq}^{(\alpha)}$ is the pqth minor of matrix α_{ij}. Numerical inspection shows that in a wide parameter range some L_m become positive. This implies the long-wavelength instability of the underlying multilayer film flow. This surface-tension-driven instability appears due to interaction between the advective (matrix α_{ij}) and damping (matrix χ_{ij}) effects. A similar instability was identified by Kliakhandler & Sivashinsky (1995) in three-layer Poiseuille flows.

In the absence of surface tension the hyperbolic part of (38) will generate shock solutions. The surface tension may be regarded as a mechanism which smooths the shocks. However, in the presence of the surface-tension-driven instability found, the solutions of (38) with vanishing surface tension do not converge to the solutions of the pertinent hyperbolic system. The mathematical feasibility of such an outcome has already been ascertained by Majda & Pego (1985) for second-order parabolic systems with viscous-like damping.

The destabilizing role of surface tension is well known in jet flows (e.g. Yarin 1993). In plane flows, however, the surface tension is traditionally regarded as a stabilizing agent. Hence, one should keep in mind that the surface tension, while suppressing short-scale modes, may however destabilize multilayer flows in the long-wavelength range.

Figure 2 shows the marginal stability curves of the surface-tension-driven instability for two-layer film flows in the (m_2, H_2^0)-plane. In this case relation (42) reduces to

$$L_m = \frac{\alpha_{12}\chi_{21} - \alpha_{22}\chi_{11} + \alpha_{21}\chi_{12} - \alpha_{11}\chi_{22} + \lambda_m^{(\alpha)}(\chi_{11}+\chi_{22})}{\alpha_{11}+\alpha_{22}-2\lambda_m^{(\alpha)}}, \quad m = 1,2. \tag{43}$$

As is seen, the instability emerges when the lower layer is less viscous than the outer one. An interesting, and somewhat counterintuitive, conclusion is that two-layer flow of miscible liquids ($\gamma_2 = 0$) may be destabilized by the surface tension on the outer interface (curve 6).

In this case, however, matrix χ_{ij} has a zeroth eigenvalue and damping of short-wavelength modes is failed. Near the inner interface the flow may be regarded as a viscous analogue of the classical Kelvin–Helmholtz problem. In such system the inner interface undergoes weak short-wavelength instability (Hooper & Boyd 1983). A description of this complicated situation, however, is a much harder problem and falls beyond the scope of the present study.

Figure 3 shows typical results of a linear stability analysis for two-layer flows for surface-tension-induced instability. Relations (40), (41), and simple similarity reasons show that the following estimates characterize the instability:

$$\mathrm{Im}\,\omega \sim -k^4 \ \text{ at } \ k \gg 1, \quad \mathrm{Im}\,\omega \sim k^4 \ \text{ at } \ k \ll 1, \quad k_c \sim W^{-1/3}. \tag{44}$$

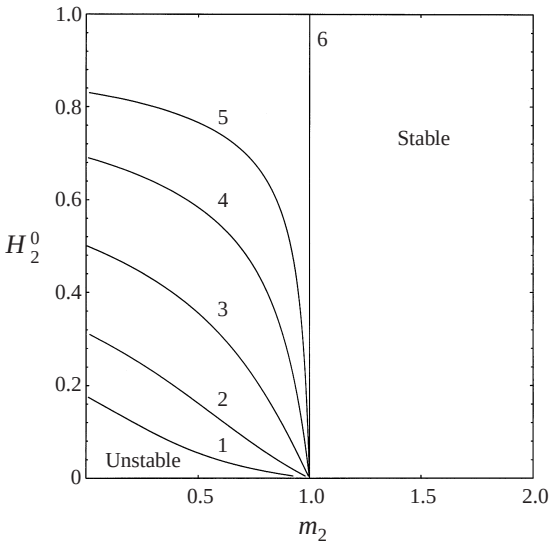

FIGURE 2. Marginal stability curves of the surface-tension-driven instability in the (m_2, H_2^0) parameter plane. Curves 1–6 correspond to W_2 $W_1 = \gamma_2 = 16, 4, 1, 1/4, 1/16, 0$ respectively.

Here k_c is the wavenumber of the most unstable mode, figure 3(a). As follows from figure 3, the instability is convective: all unstable modes travel with finite velocities. Another outcome from figure 3(b) is that (38) contain weak dispersion: group and phase velocities depend slightly on wavenumber k.

Both matrices α_{ij} and χ_{ij} depend on whole flow field. It seems therefore that the surface-tension-driven instability cannot be attributed to local mechanisms near the interfaces. To understand the instability, consider the following linearized version of (38):

$$\frac{\partial}{\partial t}\begin{pmatrix} h_1 \\ h_2 \end{pmatrix} + \begin{pmatrix} a & b \\ 0 & 0 \end{pmatrix} \frac{\partial}{\partial x}\begin{pmatrix} h_1 \\ h_2 \end{pmatrix} + \begin{pmatrix} \varepsilon & 0 \\ c & \varepsilon \end{pmatrix} \frac{\partial^4}{\partial x^4}\begin{pmatrix} h_1 \\ h_2 \end{pmatrix} = 0. \tag{45}$$

Here $a, b, c \simeq O(1)$, $0 < \varepsilon \ll 1, \omega = (-ak - 2\mathrm{i}\varepsilon k^4 \pm k(-a^2 + 4\mathrm{i}bck^3)^{1/2})/2$ and $\mathrm{Im}\,\omega \sim k^4$ at $k \ll 1$. This deliberately simple form of matrices α_{ij} and χ_{ij} is minimally sufficient for the generation of surface-tension-driven instability with damping of short modes. Simple analysis shows that two modes exist in (45). The first mode is mostly travelling and may be associated with first interface, whereas the second mode is mostly standing and may be associated with second interface. For first mode, $h_2 \simeq -\mathrm{i}ck^3 h_1/a$, and therefore the second interface is only slightly stirred with phase shift $\pm\pi/2$. For the second mode, $h_2 \simeq h_1 ca/(bc - 2a\varepsilon) + \mathrm{i}h_1 ck^3/a$. Therefore, the interfaces have almost opposite phases, being of the same order of magnitude. This second type of excitation is realized for real film flows. The crucial point here is that $\Lambda = |bc/a\varepsilon| > 1$. The numerator of Λ measures the coupling between interfaces, since b and c are on the skew diagonals in matrices α_{ij} and χ_{ij}, respectively. The denominator of Λ measures the self-interaction of the interfaces. Hence, if $\Lambda > 1$, or the coupling is sufficiently strong, the system becomes unstable.

The nonlinear dynamics of (38) was studied by direct numerical simulations. Throughout this study, nonlinear evolution equations were simulated for periodic boundary conditions. The pseudo-spectral technique was employed for the spatial discretization and the Adams–Bashforth scheme for the time advance. The standard routines C06EAF and C06EBF for the FFT, and D02CBF for the Adams–Bashforth

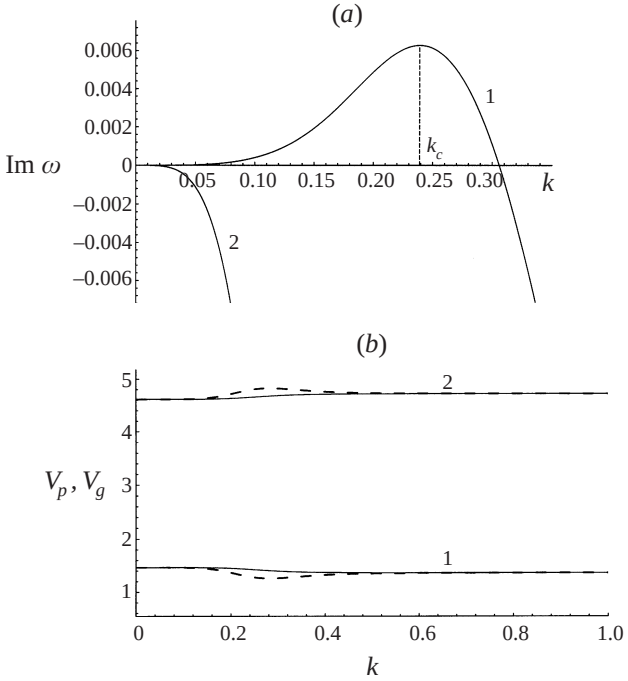

FIGURE 3. Results of a study of the linear stability problem for two-layer creeping flow of a vertically falling film for the surface-tension-driven instability: (*a*) typical growth rate $\mathrm{Im}\,\omega$ dependence on wavenumber k, (*b*) typical group $V_g = \partial\omega_r/\partial k$ (dashed line) and phase $V_p = \omega_r/k$ (solid line) velocities vs. wavenumber k. Parameters of the flow are $r_2 = 1$, $m_2 = 0.3$, $H_2^0 = 0.3$, $W_1 = W_2 = 100$ ($\gamma_2 = 1$).

scheme from the NAG routine library were implemented. The number of spatial discretization points was chosen such that the typical wavelength $\lambda_c = 2\pi/k_c$ was covered by at least 12 points (in most cases more than 20 points per λ_c were used), which ensures fair resolution of the solutions computed. The time step was chosen automatically. As initial data in all simulations, random fields or smooth functions were used. The length of the spatial interval was taken to be $10\lambda_c$.

Figure 4 shows typical results of numerical simulation of (38) under the surface-tension-induced instability for two-layer flow. The typical spatial scale of the waves is close to λ_c obtained from the linear stability analysis. The interfaces assume a varicose-like (out-of-phase), perfectly synchronized shape moving with constant velocity without change. The frame speed is close to the pertinent group velocity of the first unstable mode on figure 3 at k_c. As follows from figure 4, (38) apparently admit stable solutions in the form of periodic travelling waves. The possible formation mechanism of these travelling waves is a combination of the peak-like growth rate function of figure 3(*a*), and the presence of weak dispersion. As a result, the most unstable mode survives; all other modes are slaved by the leading mode as a consequence of their relatively weak instability rate and some dispersion.

For the case described $W_1 = W_2 = 100$, and matrices $\alpha_{ij}, \beta_{ijk}, \chi_{ij}$ are

$$\alpha_{ij} = \begin{pmatrix} 4.38 & 2.28667 \\ 0.3 & 1.7 \end{pmatrix}, \quad \beta_{1jk} = \begin{pmatrix} 3.4 & 3.26667 \\ 3.26667 & -3.26667 \end{pmatrix}, \tag{46}$$

$$\beta_{2jk} = \begin{pmatrix} 0 & 1 \\ 1 & 2.3333 \end{pmatrix}, \quad \chi_{ij} = \begin{pmatrix} 1.68867 & 0.27 \\ 0.27 & 0.06 \end{pmatrix}. \tag{47}$$

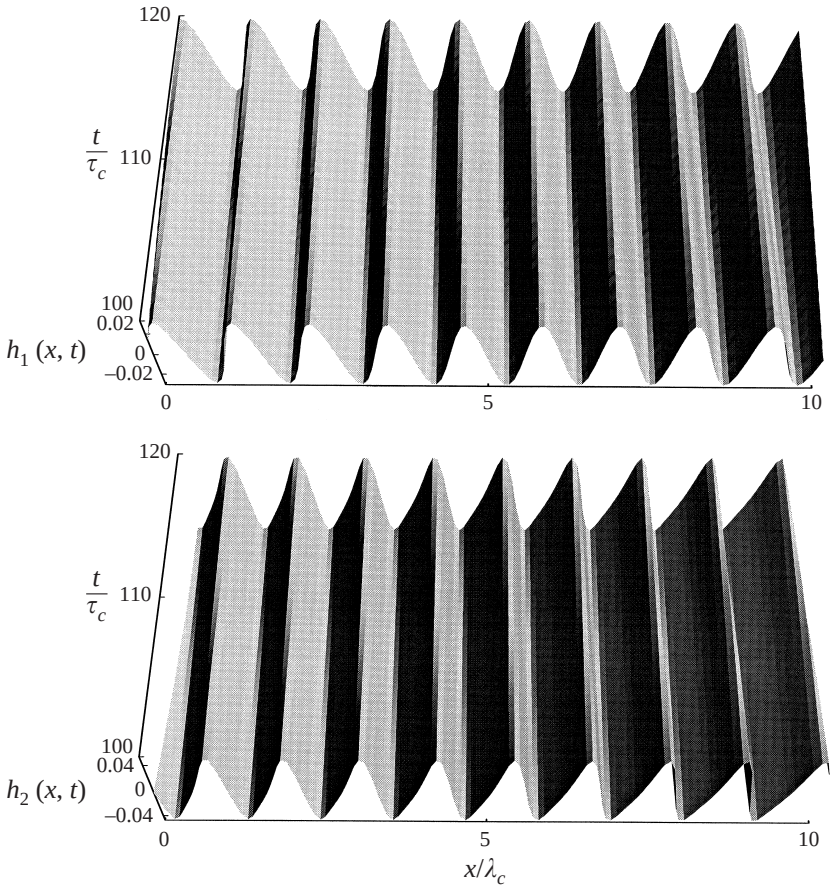

FIGURE 4. Interfaces from (38) for two-layer flow in a reference frame moving with speed 1.449. Parameters of the flow are identical to those of figure 3. Here $\tau_c = 1/\mathrm{Im}\,\omega(k_c)$ is the typical time of growth of the most unstable mode.

For three-layer flows the following interesting effect was identified: depending on initial conditions, the interfaces may acquire forms different from the perfectly synchronized periodic travelling waves. For instance, a nearly periodic form, figure 5(*a*), or an irregular form, figure 5(*b*), may be reached. In both cases, the typical length scale of the waves is close to λ_c, the interfaces vary slightly in time, and interfacial synchronization is not perfect. However, the differences in the shape of the interfaces and in the distribution of energy in spectra are preserved for a long time. In particular, the irregular interfaces at figure 5(*b*) involve a plateau. This implies that for three-layer flows (38) apparently admit several attractors.

5. Influence of destabilizing density stratification

To demonstrate the role of buoyancy variations, examine the creeping flow of a multilayer film with destabilizing (heavy-top) density stratification ($r_n < r_{n-1} < \cdots < r_1 = 1$) over an inclined plane. Equations (32) result in the following model:

$$\frac{\partial h_i}{\partial t} + \alpha_{ij}\frac{\partial h_j}{\partial x} + \beta_{ijk}\frac{\partial h_j h_k}{\partial x} + \cot\theta\ \vartheta_{ij}\frac{\partial^2 h_j}{\partial x^2} + W\chi_{ij}\frac{\partial^4 h_j}{\partial x^4} = 0. \tag{48}$$

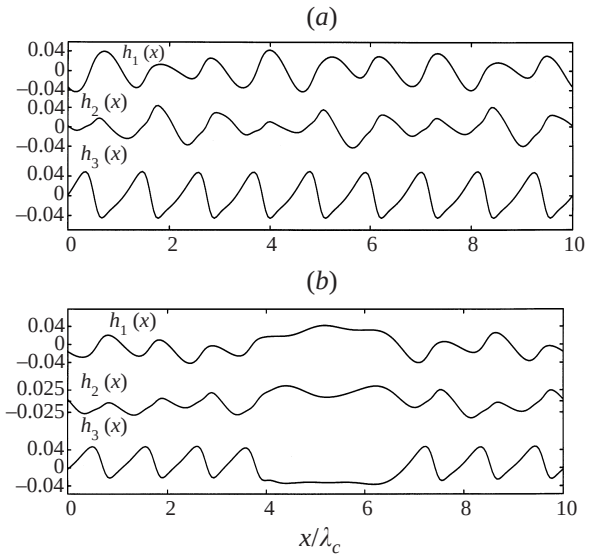

FIGURE 5. Snapshots of interfaces from (38) for three-layer flow acquiring two different states. Parameters of the flow are $r_2 = 2$, $r_3 = 3$, $m_2 = 0.7$, $m_3 = 0.3$, $H_2^0 = 0.7$, $H_3^0 = 0.3$, $W_1 = W_2 = W_3 = 100\,(\gamma_2 = \gamma_3 = 1)$.

Consider the linear stability problem for (48). Substituting $h_i = a_i \exp[\mathrm{i}(kx - \omega t)]$ in the linearized version of (48) leads to the following eigenvalue problem:

$$\mathrm{i}\omega a_i = (\mathrm{i}k\alpha_{ij} - \cot\theta\; k^2\vartheta_{ij} + Wk^4\chi_{ij})a_j. \tag{49}$$

As before, eigenvalues $\lambda^{(\alpha)}$ of matrix α_{ij} are assumed to be real.

A numerical check shows that matrix ϑ_{ij} has real positive eigenvalues for the heavy-top stratification. This is evidence of the predisposition of such systems to the Rayleigh–Taylor instability. Nevertheless, careful analysis shows that in spite of heavy-top stratification, the Rayleigh–Taylor instability in (48) and (49) may be completely suppressed.

To clarify the situation, consider the long-wavelength expansion of problem (49),

$$\omega_m \sim\; k\lambda_m^{(\alpha)} + \mathrm{i}\mathscr{C}_m k^2, \quad \mathscr{C}_m = \mathscr{L}(\alpha_{ij}, \vartheta_{ij})_m, \quad m = 1, \ldots, n, \quad k \ll 1. \tag{50}$$

Here the operator $\mathscr{L}$ is defined by (42).

For positive $\mathscr{C}$ (50) implies the emergence of the Rayleigh–Taylor type instability. Note that in two-layer Couette and Poiseuille flows with a single interface, the parameter $\mathscr{C}$ is proportional to the density jump. Therefore, for the two-layer heavy-top shear flows $\mathscr{C} > 0$ and the Rayleigh–Taylor instability is inevitably induced.

However, in multilayer film flows $\mathscr{C}$ depends both on the advective, α_{ij}, and buoyancy terms, ϑ_{ij}. Numerical inspection shows that even for the heavy-top stratification all $\mathscr{C}_m$ may become negative. This implies that in the long-wavelength range the Rayleigh–Taylor instability of heavy-top stratified film may be suppressed due to interaction of buoyancy forces and shear effects. Figure 6 shows the curves $\mathscr{C} = 0$ in the (m_2, H_2^0) parameter plane for two-layer heavy-top stratified film. The range with $\mathscr{C} < 0$ appears to be rather wide even though the upper liquid is five times more dense than the lower one.

As a result, a heavy-top multilayer system may be entirely stable due to the additional impact of surface tension. Figure 7 shows a typical plot of $\mathrm{Im}\,\omega$ vs. k for

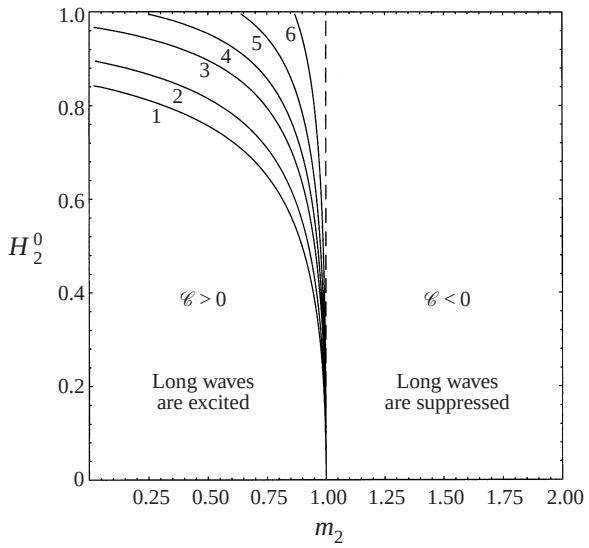

FIGURE 6. The curves $\mathscr{C} = 0$ for the Rayleigh–Taylor-type instability in a two-layer heavy-top stratified film. Curves 1–6 correspond to $r_2 = 0.2$, 0.4, 0.6, 0.7, 0.8, 0.9 respectively. Dashed line corresponds to $r_2 = 1$.

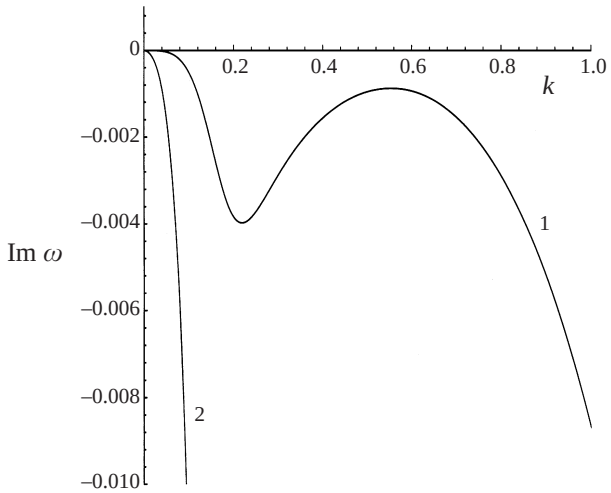

FIGURE 7. Heavy-top linearly stable two-layer system. The flow parameters are $\theta = \pi/4$, $r_2 = 0.5$, $m_2 = 0.8$, $H_2^0 = 0.8$, $W_1 = 100$, $W_2 = 1$ ($\gamma_2 = 0.01$).

heavy-top stratified flow with suppressed Rayleigh–Taylor instability. For $k \ll 1$, the flow is stable, $\mathrm{Im}\,\omega < 0$, since $\mathscr{C} < 0$. Furthermore, the destabilizing impact of the heavy-top stratification reduces the damping rate of shorter modes, $k \sim 0.4$–0.6 in figure 7. Yet the surface tension overcomes this trend. As a result, all modes become stable.

As already mentioned, two-layer single-interface shear flows with heavy-top stratification are subject to the Rayleigh–Taylor instability. Interaction of the instability with the surface tension and nonlinear effects leads to the KS equation and nonlinear saturation of unstable modes (Babchin *et al.* 1983). In contrast to that, in multilayer

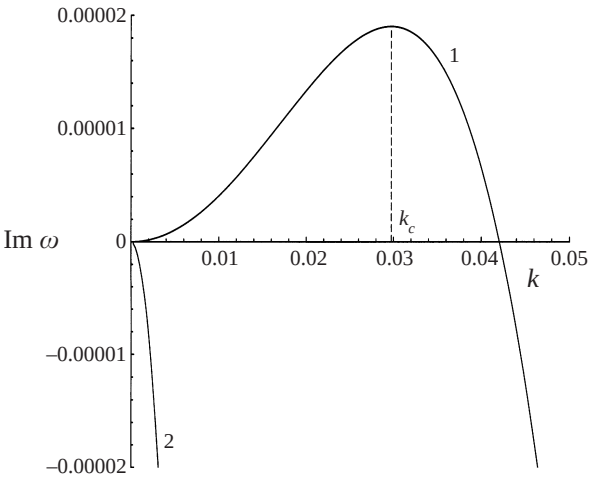

FIGURE 8. Growth rate $\mathrm{Im}\,\omega$ vs. wavenumber k in two-layer heavy-top system for the Rayleigh–Taylor-type instability, damped by the surface tension. Parameters of the flow are $\theta = \pi/4$, $r_2 = 0.6$, $m_2 = 0.2$, $H_2^0 = 0.6$, $W_1 = W_2 = 100\,(\gamma_2 = 1)$.

multi-interface film flows the Rayleigh–Taylor instability, due to a curious interaction of advective, buoyancy and surface tension effects, may be completely suppressed.

Note however that heavy-top stratified film flow will be apparently unstable in the transversal direction which is not considered here.

Let us investigate the case when the Rayleigh–Taylor-type instability is induced. In this case growth rate $\mathrm{Im}\,\omega \sim k^2$. Short-scale modes are damped as k^4 due to surface tension. Figure 8 shows the pertinent solution of the eigenvalue problem (49). The instability is convective: all unstable modes travel with finite velocities (plots of group and phase velocities are similar to those on figure 3(*b*), and are not presented here). A similar dependence $\mathrm{Im}\,\omega(k)$ appears for the single KS equation.

Figure 9 shows typical spatio-temporal evolution of the interfaces for the heavy-top stratification in a moving reference frame. The frame speed is close to the pertinent group velocity of the first unstable mode at k_c, similar to the dynamics on figures 4 and 3. For this case $W_1 = W_2 = 100, \theta = \pi/4$, and matrices $\alpha_{ij}, \beta_{ijk}, \vartheta_{ij}, \chi_{ij}$ are

$$\alpha_{ij} = \begin{pmatrix} 8 & -0.4 \\ 1.8 & 2.76 \end{pmatrix}, \quad \beta_{1jk} = \begin{pmatrix} 6.8 & 2 \\ 2 & -4 \end{pmatrix}, \quad \beta_{2jk} = \begin{pmatrix} 0 & 3 \\ 3 & -0.4 \end{pmatrix}, \tag{51}$$

$$\vartheta_{ij} = \begin{pmatrix} -3.16267 & 0.576 \\ -1.44 & 0.288 \end{pmatrix}, \quad \chi_{ij} = \begin{pmatrix} 3.16267 & 1.44 \\ 1.44 & 0.72 \end{pmatrix}. \tag{52}$$

The shape of the waves is similar to that of the single KS equation (Shraiman 1986). The interfaces are perfectly synchronized. Since the instability rate is quite small in this case, figure 8, the waves are saturated at small amplitude. The typical length scale of the waves is close to λ_c, i.e. to predictions of linear stability analysis. The time scale of wave modulations is of order of a few $\tau_c = 1/\mathrm{Im}\,\omega(k_c)$, i.e. of the same order as in the single KS equation.

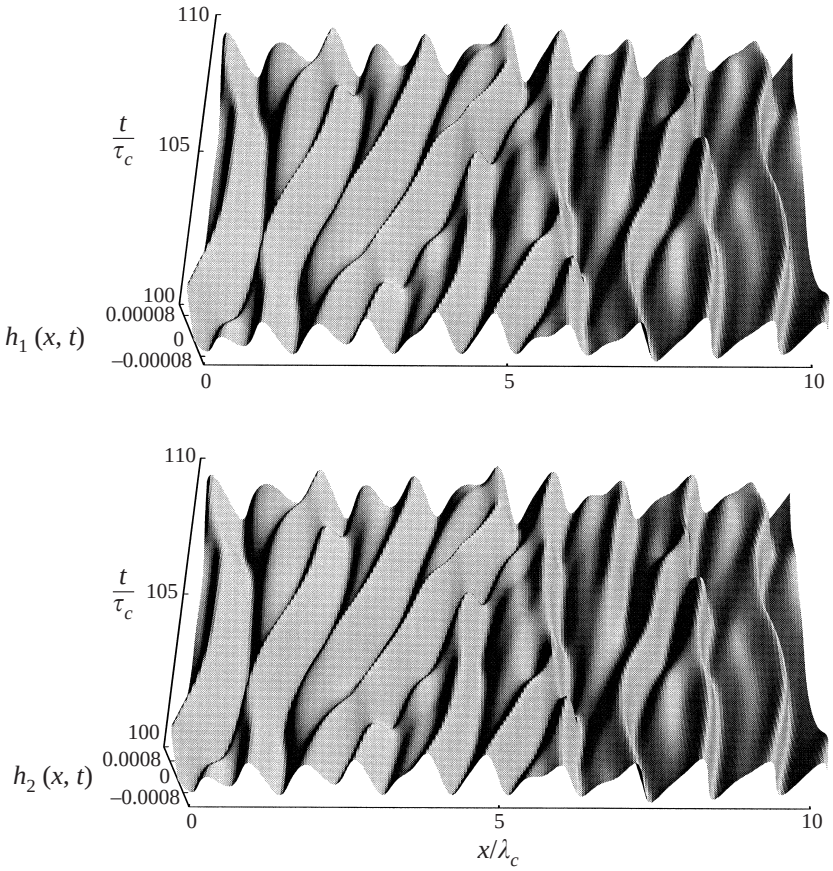

FIGURE 9. Spatio-temporal interfacial evolution described by (48) for the heavy-top flow in the reference frame moving with speed 2.051. The flow parameters are identical to those of figure 8.

6. Inertia effects

The impact of inertia may be studied in its simplest form for the multilayer film falling down a vertical wall. Equations (32) acquire the following form:

$$\frac{\partial h_i}{\partial t} + \alpha_{ij}\frac{\partial h_j}{\partial x} + \beta_{ijk}\frac{\partial h_j h_k}{\partial x} + R\sigma_{ij}\frac{\partial^2 h_j}{\partial x^2} + W\chi_{ij}\frac{\partial^4 h_j}{\partial x^4} = 0. \tag{53}$$

The linear stability analysis of (53) shows that inertia invariably exerts a destabilizing influence,

$$\mathrm{Im}\,\omega \sim \mathscr{K} Rk^2, \quad \mathscr{K} = \mathscr{L}(\alpha_{ij}, \sigma_{ij}) > 0 \tag{54}$$

(the operator $\mathscr{L}$ is defined in (42)). This kind of inertia-induced instability is the same as found by Benjamin (1957) and Yih (1963) for the flow of a homogeneous film, and was reported by Kao (1965*a*, *b*, 1968) for two-layer film flows.

Figure 10 shows typical dependences of the temporal growth rate $\mathrm{Im}\,\omega$ on wave number k for a two-layer falling film. As for previous instabilities, this instability is convective.

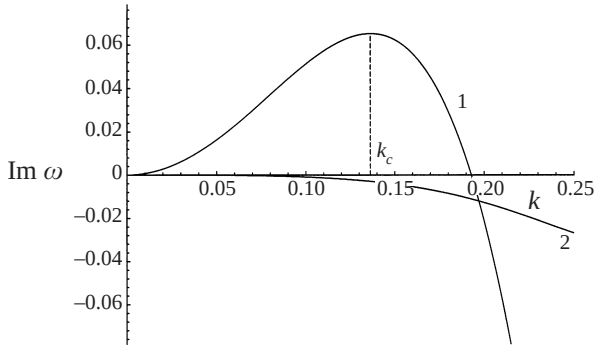

FIGURE 10. Typical dependence of the growth rate $\mathrm{Im}\,\omega$ on wavenumber k in two-layer vertically falling films for the inertia-induced instability. Parameters of the flows are $r_2 = 1$, $m_2 = 0.4$, $H_2^0 = 0.6$, $R = 1$, $W_1 = W_2 = 100$.

The results of numerical simulations of (53) are shown on figure 11. For this case $R = 1, W_1 = W_2 = 100$, and matrices $\alpha_{ij}, \beta_{ijk}, \vartheta_{ij}, \chi_{ij}$ are

$$\alpha_{ij} = \begin{pmatrix} 4.52 & 0.48 \\ 0.9 & 2.1 \end{pmatrix}, \quad \beta_{1jk} = \begin{pmatrix} 3.8 & 1.2 \\ 1.2 & -1.2 \end{pmatrix}, \quad \beta_{2jk} = \begin{pmatrix} 0 & 1.5 \\ 1.5 & 1 \end{pmatrix}, \tag{55}$$

$$\sigma_{ij} = \begin{pmatrix} 6.5623 & 1.02736 \\ 2.86476 & 0.44424 \end{pmatrix}, \quad \chi_{ij} = \begin{pmatrix} 1.60267 & 0.72 \\ 0.72 & 0.36 \end{pmatrix}. \tag{56}$$

The typical length scale of the waves is close to λ_c. The instability rate is not too small, figure 10. As a result, the amplitude of the waves is larger than that in the case considered in the previous Section. Moreover, the amplitude ratio in these cases (compare, for instance, amplitudes of upper interfaces) is about $4 \times 10^{-1}/8 \times 10^{-5} \simeq 5000$, that is of the same order as the ratio of instability rates $6 \times 10^{-2}/2 \times 10^{-5} \simeq 3000$. This observation is in accordance with the statement that the growth of unstable modes is restrained by quadratic terms. It is interesting that the synchronization is not perfect in this case: though, in general, the whole structure drifts 'in phase', the lower interface exhibits independent ripples. The spatio-temporal dynamics of the upper interface is similar to the dynamics displayed by the single KS equation. At the same time, the dynamics of the lower interface is less regular than in the single KS equation. The difference between dynamics shown on figures 11 and 9 stems seemingly from the fact that the second mode on figure 10 is damped much more slowly than on figure 8.

7. Summary

In the present work, the following results have been obtained.

The coupled nonlinear Benney equation for multilayer stratified downflowing films incorporating kinetic, buoyancy, inertia, and surface tension effects is

$$\frac{\partial H_i}{\partial t} + \frac{\partial}{\partial x}\left[Q_i + \left(\cot\theta\ G_{ij} + RT_{ij}\right)\frac{\partial H_j}{\partial x} + WF_{ij}\frac{\partial^3 H_j}{\partial x^3}\right] = 0. \tag{57}$$

The weakly nonlinear approximation of the coupled Benney equation (57) acquires

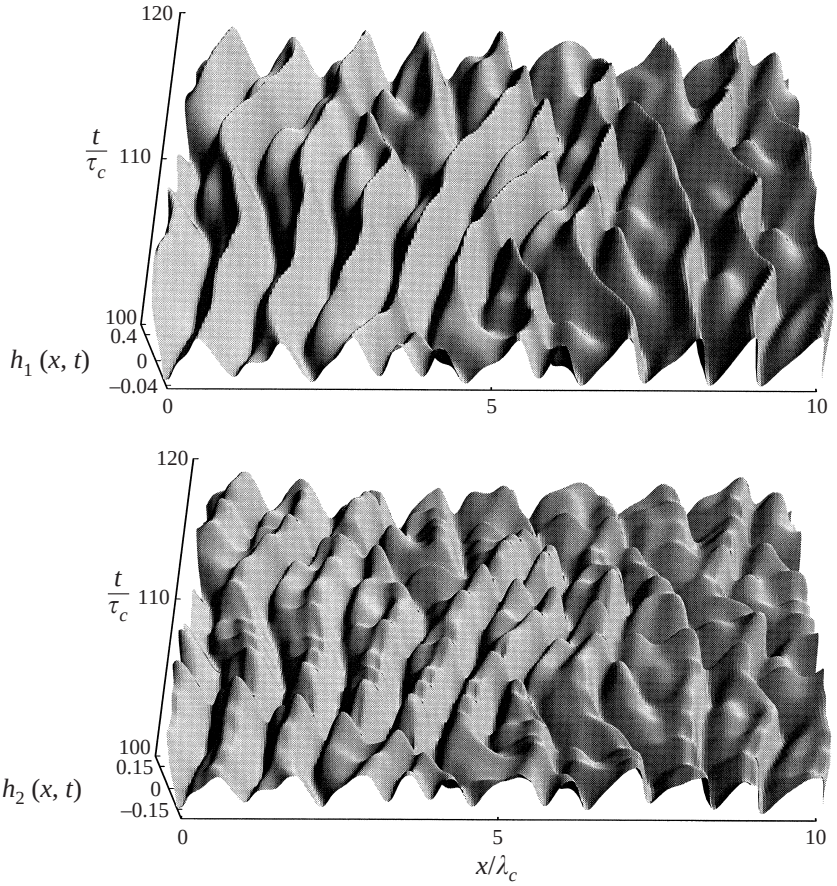

FIGURE 11. Spatio-temporal interfacial evolution described by (53) in a reference frame moving with speed 4.72. The whole structure is advected at a speed close to the associated group velocity at k_c. Parameters of the flow are identical to those of figure 10.

the form of the coupled Kuramoto–Sivashinsky (CKS) equation,

$$\frac{\partial h_i}{\partial t} + \alpha_{ij}\frac{\partial h_j}{\partial x} + \beta_{ijk}\frac{\partial h_j h_k}{\partial x} + \left(\cot\theta\ \vartheta_{ij} + R\sigma_{ij}\right)\frac{\partial^2 h_j}{\partial x^2} + W\chi_{ij}\frac{\partial^4 h_j}{\partial x^4} = 0. \tag{58}$$

To clarify the role of the terms involved, a few shortened versions of (58) have been considered.

The surface-tension-driven instability of creeping multilayer film flow down vertical wall is described by the following model

$$\frac{\partial h_i}{\partial t} + \alpha_{ij}\frac{\partial h_j}{\partial x} + \beta_{ijk}\frac{\partial h_j h_k}{\partial x} + W\chi_{ij}\frac{\partial^4 h_j}{\partial x^4} = 0. \tag{59}$$

In two-layer flows, the interfaces governed by (59) assume form of periodic travelling waves. In three-layer flows, (59) exhibit an interesting phenomenon: depending on initial conditions, the interfaces may acquire the form of nearly periodic, or irregular waves.

The CKS equation for creeping film flows with unstable density stratification over an inclined plane is

$$\frac{\partial h_i}{\partial t} + \alpha_{ij}\frac{\partial h_j}{\partial x} + \beta_{ijk}\frac{\partial h_j h_k}{\partial x} + \cot\theta\ \vartheta_{ij}\frac{\partial^2 h_j}{\partial x^2} + W\chi_{ij}\frac{\partial^4 h_j}{\partial x^4} = 0. \tag{60}$$

The interfaces governed by (60) display perfect synchronization of the interfaces, and their dynamics is close to that of the single KS equation.

Finally, the dynamics of (58) incorporating the impact of inertia is somewhat different from that of the single KS equation. Loosely speaking, the interfaces are chaotic, and are not perfectly synchronized.

Numerical simulations of interfacial dynamics in other cases which are not shown here (i.e. flow with finite Reynolds number over an inclined plane, the simultaneous presence of few described instabilities, etc.), show interfacial dynamics which are more or less similar to the cases considered. The detailed investigation of observed dynamical phenomena, i.e. travelling periodic waves, the presence of a few attractors, chaotic-like patterns, perfect and imperfect synchronization, will be the subject of future works.

Note that the velocities of the interfaces in steady-state flow of multilayer film are different. Nevertheless, the wavy interfacial structures drift 'in-phase'. The outcome is that model (58), displaying different types of coherent dynamics, may serve as a model of 'collective behaviour' for strongly interacting waves.

This work was supported by the Eshkol Fund of Ministry of Science, Israel. I would like to thank H.-C. Chang, A. Frenkel, C. Kobayashi, S. Weinstein for useful comments. I indebted to A. Nepomnyashchy for stimulating and enlightening conversations. I am deeply grateful to G. Sivashinsky for numerous fruitful discussions and encouragement. The comments of Referees, which allowed the paper to be improved markedly, are much appreciated.

Appendix. The kinetic, buoyancy, surface tension and inertia terms for two-layer flows

The flow rates Q_i of two-layer flow are given by (here $m = m_2$ and $r = r_2$),

$$Q_1 = (6H_1^2H_2 - 9H_1H_2^2 + 3H_2^3 + 2H_1^3m - 6H_1^2H_2m + 6H_1H_2^2m - 2H_2^3m + 3H_1H_2^2r - H_2^3r)/3m, \tag{A 1}$$

$$Q_2 = H_2^2(3H_1 - 3H_2 + 2H_2r)/3m. \tag{A 2}$$

The buoyancy impact is described by the matrix G_{ij},

$$G_{11} = 2(-3H_1^2H_2 + 3H_1H_2^2 - H_2^3 - H_1^3m + 3H_1^2H_2m - 3H_1H_2^2m + H_2^3m)/3m, \tag{A 3}$$

$$G_{12} = H_2^2(-3H_1 + H_2)(r-1)/3m, \tag{A 4}$$

$$G_{21} = H_2^2(-3H_1 + H_2)/3m, \quad G_{22} = 2H_2^3(1-r)/3m. \tag{A 5}$$

The surface tension influence is described by the matrix F_{ij} (here $\gamma_2 = W_2/W_1$),

$$F_{11} = (3H_1^2H_2 - 3H_1H_2^2 + H_2^3 + H_1^3m - 3H_1^2H_2m + 3H_1H_2^2m - H_2^3m)W_1/3m, \tag{A 6}$$

$$F_{12} = \gamma_2\left((3H_1 - H_2)H_2^2W_2/3m\right), \tag{A 7}$$

$$F_{21} = (3H_1 - H_2)H_2^2W_1/3m, \quad F_{22} = 2\gamma_2H_2^3W_2/3m. \tag{A 8}$$

The inertia impact is controlled by the martix T_{ij},

$$T_{11}=\frac{8H_1^6}{15}-\frac{16H_1^5H_2}{5}+8H_1^4H_2^2-\frac{32H_1^3H_2^3}{3}+8H_1^2H_2^4-\frac{16H_1H_2^5}{5}+\frac{8H_2^6}{15}$$
$$+\frac{6H_1^3H_2^3}{m^3}-\frac{15H_1^2H_2^4}{m^3}+\frac{12H_1H_2^5}{m^3}-\frac{3H_2^6}{m^3}+\frac{22H_1^4H_2^2}{3m^2}-\frac{80H_1^3H_2^3}{3m^2}+\frac{36H_1^2H_2^4}{m^2}$$
$$-\frac{64H_1H_2^5}{3m^2}+\frac{14H_2^6}{3m^2}+\frac{16H_1^5H_2}{5m}-\frac{46H_1^4H_2^2}{3m}+\frac{88H_1^3H_2^3}{3m}-\frac{28H_1^2H_2^4}{m}+\frac{40H_1H_2^5}{3m}$$
$$-\frac{38H_2^6}{15m}+\frac{25H_1^2H_2^4r}{6m^3}-\frac{179H_1H_2^5r}{30m^3}+\frac{9H_2^6r}{5m^3}+\frac{2H_1^3H_2^3r}{m^2}-\frac{31H_1^2H_2^4r}{6m^2}+\frac{13H_1H_2^5r}{3m^2}$$
$$-\frac{7H_2^6r}{6m^2}+\frac{5H_1H_2^5r^2}{6m^3}-\frac{3H_2^6r^2}{10m^3}, \tag{A 9}$$

$$T_{12}=\frac{-8H_1^6}{15}+\frac{16H_1^5H_2}{5}-8H_1^4H_2^2+\frac{32H_1^3H_2^3}{3}-8H_1^2H_2^4+\frac{16H_1H_2^5}{5}$$
$$-\frac{8H_2^6}{15}+\frac{4H_1^4H_2^2}{m^3}-\frac{20H_1^3H_2^3}{m^3}+\frac{33H_1^2H_2^4}{m^3}-\frac{22H_1H_2^5}{m^3}+\frac{5H_2^6}{m^3}+\frac{8H_1^5H_2}{3m^2}$$
$$-\frac{20H_1^4H_2^2}{m^2}+\frac{152H_1^3H_2^3}{3m^2}-\frac{176H_1^2H_2^4}{3m^2}+\frac{32H_1H_2^5}{m^2}-\frac{20H_2^6}{3m^2}+\frac{8H_1^6}{15m}-\frac{32H_1^5H_2}{5m}$$
$$+\frac{70H_1^4H_2^2}{3m}-\frac{40H_1^3H_2^3}{m}+\frac{36H_1^2H_2^4}{m}-\frac{248H_1H_2^5}{15m}+\frac{46H_2^6}{15m}+\frac{22H_1^3H_2^3r}{3m^3}-\frac{67H_1^2H_2^4r}{3m^3}$$
$$+\frac{203H_1H_2^5r}{10m^3}-\frac{53H_2^6r}{10m^3}+\frac{10H_1^4H_2^2r}{3m^2}-\frac{44H_1^3H_2^3r}{3m^2}+\frac{139H_1^2H_2^4r}{6m^2}-\frac{47H_1H_2^5r}{3m^2}$$
$$+\frac{23H_2^6r}{6m^2}+\frac{8H_1^5H_2r}{15m}-\frac{8H_1^4H_2^2r}{3m}+\frac{16H_1^3H_2^3r}{3m}-\frac{16H_1^2H_2^4r}{3m}+\frac{8H_1H_2^5r}{3m}-\frac{8H_2^6r}{15m}$$
$$+\frac{25H_1^2H_2^4r^2}{6m^3}-\frac{34H_1H_2^5r^2}{5m^3}+\frac{21H_2^6r^2}{10m^3}+\frac{2H_1^3H_2^3r^2}{3m^2}-\frac{2H_1^2H_2^4r^2}{m^2}$$
$$+\frac{2H_1H_2^5r^2}{m^2}-\frac{2H_2^6r^2}{3m^2}+\frac{5H_1H_2^5r^3}{6m^3}-\frac{3H_2^6r^3}{10m^3}, \tag{A 10}$$

$$T_{21}=\frac{3H_1^2H_2^4}{m^3}-\frac{6H_1H_2^5}{m^3}+\frac{3H_2^6}{m^3}+\frac{8H_1^3H_2^3}{3m^2}-\frac{8H_1^2H_2^4}{m^2}+\frac{8H_1H_2^5}{m^2}-\frac{8H_2^6}{3m^2}+\frac{2H_1^4H_2^2}{3m}$$
$$-\frac{8H_1^3H_2^3}{3m}+\frac{4H_1^2H_2^4}{m}-\frac{8H_1H_2^5}{3m}+\frac{2H_2^6}{3m}+\frac{71H_1H_2^5r}{30m^3}-\frac{71H_2^6r}{30m^3}$$
$$+\frac{5H_1^2H_2^4r}{6m^2}-\frac{5H_1H_2^5r}{3m^2}+\frac{5H_2^6r}{6m^2}+\frac{8H_2^6r^2}{15m^3}, \tag{A 11}$$

$$T_{22}=\frac{2H_1^3H_2^3}{m^3}-\frac{9H_1^2H_2^4}{m^3}+\frac{12H_1H_2^5}{m^3}-\frac{5H_2^6}{m^3}+\frac{2H_1^4H_2^2}{3m^2}-\frac{16H_1^3H_2^3}{3m^2}$$
$$+\frac{12H_1^2H_2^4}{m^2}-\frac{32H_1H_2^5}{3m^2}+\frac{10H_2^6}{3m^2}-\frac{2H_1^4H_2^2}{3m}+\frac{8H_1^3H_2^3}{3m}-\frac{4H_1^2H_2^4}{m}+\frac{8H_1H_2^5}{3m}-\frac{2H_2^6}{3m}$$
$$+\frac{23H_1^2H_2^4r}{6m^3}-\frac{301H_1H_2^5r}{30m^3}+\frac{31H_2^6r}{5m^3}+\frac{2H_1^3H_2^3r}{3m^2}-\frac{17H_1^2H_2^4r}{6m^2}+\frac{11H_1H_2^5r}{3m^2}-\frac{3H_2^6r}{2m^2}$$
$$+\frac{71H_1H_2^5r^2}{30m^3}-\frac{29H_2^6r^2}{10m^3}+\frac{8H_2^6r^3}{15m^3}. \tag{A 12}$$

REFERENCES

Akhtaruzzaman, A. F., Wang, C. K. & Lin, S. P. 1978 Wave motion in multilayered liquid films. *J. Appl. Mech.* **45**, 25–31.

Babchin, A. J., Frenkel, A. L., Levich, B. G. & Sivashinsky, G. I. 1983 Nonlinear saturation of Rayleigh–Taylor instability in thin films. *Phys. Fluids* **26**, 3159–3161.

Benjamin, T. B. 1957 Wave formation in laminar flow down an inclined plane. *J. Fluid Mech.* **2**, 554–574; and Corrigendum **3**, 657.

Benney, D. J. 1966 Long waves on liquid films. *J. Math. Phys.* **45**, 150–155.

Chang, H.-C. 1994 Wave evolution on a falling film. *Ann. Rev. Fluid Mech.* **26**, 103–136.

Chen, K. P. 1993 Wave formation in the gravity-driven low-Reynolds number flow of two liquid films down an inclined plane. *Phys. Fluids* A **5**, 3038–3048.

Cohen, B. I., Krommes, J. A., Tang, W. M. & Rosenbluth, M. N. 1976 Non-linear saturation of the dissipative trapped-ion mode by mode coupling. *Nucl. Fusion* **16**, 971–992.

Cross, M. C. & Hohenberg, P. C. 1993 Pattern formation outside of equilibrium. *Rev. Mod. Phys.* **65**, 851–1112.

Homsy, G. M. 1974 Model equations for wavy viscous film flow. Lectures in Applied Mathematics: *Nonlinear wave motion* **15**, 191–194.

Hooper, A. P. & Boyd, G. C. 1983 Shear-flow instability at the interface between two viscous fluids. *J. Fluid Mech.* **128**, 507–528.

Hooper, A. P. & Grimshaw, R. 1985 Nonlinear instability at the interface between two viscous fluids. *Phys. Fluids* **28**, 37–45.

Joseph, D. D. & Renardy, Y. 1993 *Fundamentals of Two-Fluid Dynamics.* vols. I, II. Springer.

Kao, T. W. 1965*a* Stability of two-layer viscous stratified flow down an inclined plane. *Phys. Fluids* **8**, 812–820.

Kao, T. W. 1965*b* Role of the interface in the stability of stratified flow down an inclined plane. *Phys. Fluids* **8**, 2190–2194.

Kao, T. W. 1968 Role of viscosity stratification in the stability of two-layer flow down an incline. *J. Fluid Mech.* **33**, 561–572.

Kliakhandler, I. L. & Sivashinsky, G. I. 1995 Kinetic alpha effect in viscosity stratified creeping flows. *Phys. Fluids* **7**, 1866–1871.

Kliakhandler, I. L. & Sivashinsky, G. I. 1997 Viscous damping and instabilities in stratified liquid film flowing down a slightly inclined plane. *Phys. Fluids* **9**, 23–30.

Kobayashi, C. 1992 Stability analysis of film flow on an inclined plane I. One layer, two-layer flow. *Indust. Coating Res.* **2**, 65–88.

Kobayashi, C. 1995 Stability analysis of film flow on an inclined plane II. Multi-layer flow. *Indust. Coating Res.* **3**, 103–125.

Kuramoto, Y. & Tsuzuki, T. 1976 Persistent propagation of concentration waves in dissipative media far from thermal equilibrium. *Prog. Theor. Phys.* **55**, 356–369.

Kurz, M. R., Weinstein, S. J. & Ruschak, K. J. 1994 Method of coating multilayer photographic elements with reduced ripple defects. US Patent No. 5,306,527.

Lin, S. P. 1983*a* Film waves. In *Waves on Fluid Interfaces* (ed. R. P. Meyer), pp. 261–289. Academic.

Lin, S. P. 1983*b* Effects of surface solidification on the stability of multi-layered liquid films. *J. Fluids Engng* **105**, 119–1120.

Loewenherz, D. S. & Lawrence, C. J. 1989 The effect of viscosity stratification on the stability of a free surface flow at low Reynolds number. *Phys. Fluids* A **1**, 1686–1693.

Majda, A. & Pego, R. L. 1985 Stable viscosity matrices for systems of conservation laws. *J. Diffl Equat.* **56**, 229–262.

Mei, C. C. 1966 Nonlinear gravity waves in a thin sheet of viscous fluid. *J. Math. Phys.* **45**, 266–288.

Nepomnyashchy, A. A. 1974 Stability of wave regimes in a film flowing down on inclined plane. *Fluid Dyn.* **9**, 354–359.

Shlang, T., Sivashinsky, G. I., Babchin, A. J. & Frenkel, A. L. 1985 Irregular wavy flow due to viscous stratification. *J. Phys. Paris* **46**, 863–866.

Shraiman, B. S. 1986 Order, disorder, and phase turbulence. *Phys. Rev. Lett.* **57**, 325–328.

Sivashinsky, G. I. 1977 Nonlinear analysis of hydrodynamic instability of laminar flames. Part 1. Derivation of basic equations. *Acta Astronautica* **4**, 1177–1206.

WANG, S. K., SEABORG, J. J. & LIN, S. P. 1978 Instability of multi-layered liquid films. *Phys. Fluids* **21**, 1669–1673.

WEINSTEIN, S. J. & KURZ, M. R. 1991 Long-wavelength instabilities in three-layer flow down an incline. *Phys. Fluids* A **3**, 2680–2687.

YARIN, A. L. 1993 *Free Liquid Jets and Films*. Longman.

YIH, C. 1963 Stability of liquid flow down an inclined plane. *Phys. Fluids* **6**, 321–330.